PHYSICAL REVIEW C VOLUME 24, NUMBER 2 AUGUST 1981

Cluster emission amplification from nuclei at high angular momenta

M. Blann and T. T. Komoto
Lawrence Livermore National Laboratory, Livermore, California 94550
(Received 7 July 1980; revised manuscript received 25 February 1981)

Predictions for statistical decay of highly deformed nuclei using the Hauser-Feshbach formulation are presented including emission of clusters up to ^{12}C. These calculatons use the rotating liquid drop model to estimate deformation versus angular momentum. The algorithms used to compute transmission coefficients for spherical and for deformed nuclei are presented, as well as results for several sets of calculations for $A = 56$ and 148 compound nuclei. Several different formulations are explored for computing decay rates of deformed nuclei. Large cluster emission amplification is predicted when deformation is considered, with consequent decrease in first chance fission. Qualitative comparisons are made with some heavy ion experiments which are consistent with these predictions, and types of experiments to verify the new cluster decay amplification mechanism are suggested. It is pointed out that the phase space dependence on deformation may prove valuable in interpreting some nonequilibrium heavy ion reaction results.

[NUCLEAR REACTIONS Model equilibrium decay clusters from superdeformed nuclei at high angular momenta. Discuss relevance new decay mode to incompletely equilibrated heavy ion systems. Compare predictions qualitatively with experimental results.]

I. INTRODUCTION

Many heavy ion reaction yields have been analyzed by comparisons with equilibrium statistical model predictions. Reaction mechanisms are often deduced from the agreement or disagreement between statistical model expectation and experimental observation. Usually the role of angular momentum was recognized in statistical model calculations by lowering the fission barriers due to deformation.[1-4] Strangely enough, the effect of this deformation has generally been overlooked with respect to particle emission rates from the deformed nuclei.

Recently, the ground state deformations predicted by the rotating liquid drop (RLD) model were used to model n, p, and α transmission coefficients $[T_l(\epsilon)]$ as a function of emitting nucleus angular momentum.[5-7] Results for the predicted decay channels were drastically altered from earlier calculations in which $T_l(\epsilon)$ computed for spherical ground state nuclei were used. Large amplifications of the α decay rates resulted for the highly deformed triaxial nuclei with consequent suppression of first chance fission.[7] If such an amplification effect had been observed experimentally it might well have been interpreted as a precompound effect if compared with predictions of the statistical model with $T_l(\epsilon)$ computed for spherical nuclei.

In this paper the earlier modeling effort for deformed nuclei has been expanded to include emission of heavier clusters—specifically ^{7}Li, ^{8}Be, ^{9}Be, ^{10}B, and ^{12}C. Several different approaches are used to calculate the decay rates in addition to the extreme assumptions used in earlier works. Results are presented compared to calculations with $T_l(\epsilon)$ modeled for spherical nuclei. As in the earlier work, the predicted course of deexcitation is altered for superdeformed nuclei. Many experimental results are qualitatively in agreement with these predicted changes; results which had been interpreted as precompound or direct reactions are now found to be consistent with compound decay expectations. Although this consistency by no means confirms a compound nucleus mechanism, it suggests that caution should be exercised before dismissing compound nucleus interpretations.

It has been shown that heavy ion compound lifetimes should become comparable to equilibration times and coalescence times at moderate excitations. In addition, experiments, supported by theoretical modeling, have shown that significant equilibration of excitation sets in very rapidly in heavy ion reactions, with significant particle emission expected during the coalescence process. In view of these observations the results to be presented in terms of fully equilibrated systems may be relevant to the equilibrating systems. They would then predict a new type of precompound decay, best described as "centrifugal fragmentation." The centrifugal fragmentation mechanism would be different from precompound decay of light-projectile induced reactions in that it results from collective (deformation) influences on phase space rather than on intrinsic excitations.

In Sec. II we describe the relevant parametrizations and decay equations used, with reference to earlier works containing more detailed descriptions of the computer codes and fission decay rates. The approximations and uncertainties of the model calculations are discussed. The phase space relationships which result in the cluster emission amplification are reviewed qualitatively. Different ways to calculate the decay rates are described.

In Sec. III, results of model calculations are presented and compared for the "old statistical model" [$T_l(\epsilon)$ for spherical nuclei] and for the new approach with respect to the angular momentum deformation dependence of $T_l(\epsilon)$. Compound nuclei in the mass 60 and 150 regions have been selected arbitrarily to illustrate the mass dependence of the results.

In Sec. III some qualitative comparisons are made between recent experimental results and the predictions of the new model. Additionally, some noncompound results are reviewed, and relevance to the present work is discussed. Section IV presents our conclusions.

II. DECAY FORMULATION AND CLUSTER EMISSION PARAMETRIZATION

A. Statistical decay code

The code used in these calculations, ALERTII, is a modification of the Hauser-Feshbach (HF) multiple particle emission code MBII.[8] These codes include fission as a deexcitation channel according to the RLD and Bohr-Wheeler models. Detailed descriptions of the treatment of the fission channel are to be found elsewhere.[3]

The emission probability for particle ν with channel energy ϵ and spin s_ν from a compound nucleus of angular momentum I to give a residual nucleus at excitation U and angular momentum J is given by

$$P_\nu(\epsilon, I)d\epsilon = \frac{(2s_\nu+1)\sum_{l=0}^{\infty}\sum_{J=|I-l|}^{I+l} {}_\nu T_l^J(\epsilon)\rho(U,J)d\epsilon}{\int_{\epsilon=0}^{\infty}\sum_{\nu=1}^{n}(2s_\nu+1)\sum_{l=0}^{\infty}\sum_{J=|I-l|}^{I+l} {}_\nu T_l^J(\epsilon)\rho(U,J)d\epsilon}. \tag{1}$$

The ${}_\nu T_l^J(\epsilon)$ represents the transmission coefficient for particle ν at channel energy ϵ to form a residual nucleus with angular momentum J and $\rho(U,J)$ the residual level density. The spin dependent level density was used in the form suggested by Lang,[9]

$$\rho(U,J) \propto (2J+1)U^{-2}\exp(2\{a[U-U_{\rm rot}(J)]\}^{1/2}), \tag{2}$$

where $U_{\rm rot}(J)$ is the energy of the rotational nucleus at angular momentum J, differing from the ground state by the rotational energy and by surface and Coulomb energies which are modified by the equilibrium deformation.

Lang demonstrated that this formulation gives a better representation of more exact level density expansions than does the commonly used exponential spin cutoff form, and goes to zero at the yrast line. The rotational energies used in (1) and (2) in this work were evaluated for the equilibrium deformations of the rigid rotors predicted by the RLD model.[1] The code included a γ-ray deexcitation channel and evaluates a space with a mesh size 1 MeV by $1\hbar$. A fission rate according to the Bohr-Wheeler formalism was also included in the denominator of Eq. (1).

The code as described[7,8] was modified to allow the emission of up to eight particle types in addition to the γ-ray and fission channels. The first two particles are always neutrons and protons. The five additional particles are specified at time of execution as to mass number, atomic number, and intrinsic spin. Results to be presented in this work considered emission of n, p, α, ^{7}Li, ^{8}Be, ^{9}Be, ^{10}B, and ^{12}C from $^{56}_{28}$Ni and $^{148}_{62}$Sm compound nuclei. Limits involved in evaluating Eq. (1) are discussed in Sec. III B; calculation of transmission coefficients is described in Secs. II C and II D.

B. Evaluation of decay rates

The point of the present work is that the very large deformations expected in compound nuclei formed in heavy ion reactions previously have been only partially incorporated into the statistical decay calculations. In particular the fission barriers have been calculated with the RLD model, and yrast energies of residual nuclei have been computed using the RLD rotational energies for deformed nuclei. Yet the T_l have been computed for spherical nuclei, and this represents an inconsistency.

Recognition of the inconsistency is less controversial than the question of how to formulate statistical decay when compound and residual nuclei each have substantially different deformations. We will therefore present results of a calculation of the type previously used in statistical codes, and three modifications intended to illustrate the possible influences of the large deformations. The physical assumptions of these calculations can be described as follows:

(A) T_l are computed for a spherical residual nucleus, but the yrast energy is calculated for the equilibrium deformed final nucleus as given by the RLD model;

(B) T_l are computed for the compound nucleus deformation predicted by RLD model, and the yrast energy is computed for the equilibrium deformed residual nucleus;

(C) T_l are computed for the compound nucleus deformation, and the yrast energies of the residual nuclei are calculated assuming that the compound nucleus deformation is a frozen (collective) degree of freedom;

(D) T_l and yrast energies are both computed for the equilibrium residual nucleus deformation.

Of these approaches, (A) is recognized as the one which has been used commonly over the past decade. It would in some sense be a more consistent formulation (but not necessarily better) if not only the T_l but also the yrast energies had been computed for spherical nuclei. Calculation (B) is the approach which has been taken in several recent works.[5-7] It has an implicit assumption that there is complete overlap in shape for the initial and final state wave functions.

It is the easiest method computationally for handling T_l for deformed nuclei and for this reason was used in works preceding this. However, the phase space is calculated with T_l based on compound nucleus shape, and the final state level density based on residual nucleus deformation. The total phase space is not computed at a single point, and while computationally convenient it is physically incorrect.

Formulation (C) assumes that there is no readjustment of shape of the nascent final nucleus towards its equilibrium deformation at the saddle point consisting of final nucleus plus ejectile just outside the range of nuclear forces. Moretto has previously presented a saddle point formulation for statistical decay of clusters and nucleons, for somewhat different reasons.[10]

Formulation (D) results from a detailed balance approach where the decay rate is based on the capture rate of the ejectile by the equilibrium deformed residual nucleus. Using the residual nucleus deformation is a conservative method of limiting the T_l range; this limit should provide the physical information as to the overlap restrictions between initial and final states.

The phase space relationships of the several calculations may be seen in Fig. 1, which is an excitation energy versus angular momentum diagram for a ^{56}Ni compound nucleus at 176 MeV of excitation with 55$\hbar$ of angular momenta. The curves *AD* and *GI* represent the loci of minimum angular momenta which may be populated in the residual nucleus by α emission if the T_l are computed for spherical (*AD*) or deformed (*IG*) nuclei (compound nucleus deformation is assumed). Curves are shown for the yrast lines computed for a spherical rigid rotor, for the RLD yrast line of the equilibrium deformed residual nucleus, and for the yrast line based on the compound nucleus deformation.

The decay rates as given by Eq. (1) are given by the summation (over *J* values) for level densities of Eq. (2) which are evaluated for the excitation energies above the appropriate yrast energies. Thus for calculation (A), the area bounded by ACFD enters the decay rate result as lower limits in the summation over *J*. If a spherical

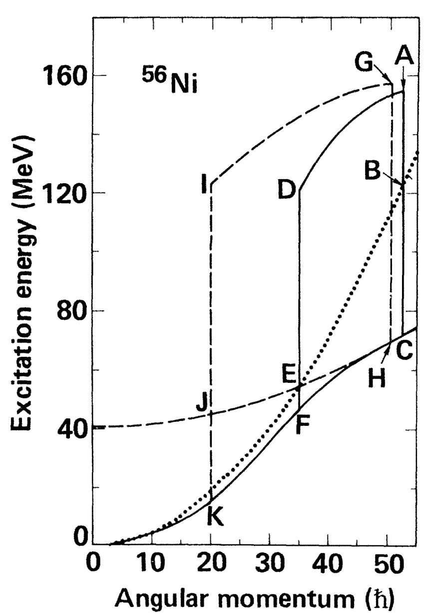

FIG. 1. Energy and angular momentum space for statistical deexcitation of a ^{56}Ni compound nucleus at 55$\hbar$ and 176 MeV excitation energy. The dotted curve represents the rigid spherical rotor yrast line, the lower solid curve represents the RLD model yrast line, and the lower dashed curve represents the RLD yrast line for a nucleus having the shape (and moment of inertia) predicted by the RLD model for a nucleus at 55$\hbar$. The relationship of these several yrast limits to decay rates is discussed in the text.

rotor had been assumed rather than the RLD model result, then the curve ABED would have bounded the relevant area. Calculation (B) involves limits in Eq. (1) given by GHKI; it may be seen that this represents the maximum area of the possible approaches, and therefore will give the maximum effects on decay rates. Calculation (C) involves limits given by GHJI.

Calculation (D) should give a residual nucleus J locus somewhere between AD and GI, with level densities computed from the equilibrium residual nucleus yrast line. One should remember that the deformation enters the fission rate only via the compound nucleus fission barrier, so that the fission rate is the same for all approaches (A)–(D). However, as particle emission rates change, the fission probability will change due to the competition with particle emission.

We have presented several options as to how to model deformation into decay rates. Recommendations as to the most appropriate are more difficult to make, as they depend on the dynamical influence on the potential energy surface as the particle is just being emitted from the compound nucleus. We would expect calculation (B) to overestimate the deformation effects, as a total overlap between initial and final state shapes is highly unlikely. Calculation (C), on the other hand, requires a complete overlap of shapes by freezing this degree of freedom; no change of collective to intrinsic excitation upon particle emission is assumed and this therefore seems a safe and conservative approach to the problem.

Viewing the decay process as an equilibrium phenomenon with time reversal leads to calculation (D); however, the question of the evaluation of the T_l which can connect different initial and final states is more difficult when the usual assumed spherical symmetry is not present; once again the question of dynamics enters. In this context calculation (D) is again conservative, as the lower residual nucleus deformations rather than the larger deformations of the compound nuclei are used in defining the limiting ejectile orbital angular momenta; this imposes the limit on overlap of shapes which is missing in calculation (B). We would conclude that the effects predicted in calculating (C) and (D) should be very reasonable, with larger effects possible, if the nuclear shape can change significantly during the particle emission process.

C. Transmission coefficients for spherical nuclei

The $T_l(\epsilon)$ used in this work were based on a classical sharp cutoff (SCO) model. For the n, p, and α channels the SCO parameters were selected to approximately reproduce the $T_l = 0.5$ loci of the nuclear optical model. The latter used the global parameter sets contained with the optical model subroutine of the code ALICE.[11-14] Comparisons between the SCO and optical model results were presented in Ref. 7. For heavier clusters the parametrization of $T_l(\epsilon)$ for α particles was modified in a consistent fashion as will be described.

The radius R of a residual nucleus following emission of a particle of mass number ν from a nucleus of mass number $A_{\rm CN}$ was taken to be

$$R = 1.21(A_{\rm CN} - \nu)^{1/3} \tag{3}$$

and the radius of the particle ν was taken to be

$$R_\nu = 1.21(\nu)^{1/3}\,. \tag{4}$$

For spherical nuclei the maximum angular momentum (l_m) which could be carried off by a neutron was taken to be

$$l_m = 0.187(2\mu\epsilon)^{1/2}\,[R + R_\nu + 3.4/(\epsilon + 0.4)^{1/2}]\,, \tag{5}$$

where ϵ is the channel energy in MeV and μ is the reduced mass.

For charged particles,

$$l_m = 0.187\,[2\mu\epsilon(1 - V_\nu/\epsilon)]^{1/2} \tag{6}$$

where the Coulomb barrier V_ν (MeV) is given by

$$V_\nu = \frac{(Z - Z_\nu)Z_\nu K_\nu}{(R + R_\nu + 1.6)}\,, \tag{7}$$

and where Z is the compound nucleus atomic number, Z_ν is the cluster atomic number, K_ν is a constant, and 1.6 is a finite range parameter. The value of K_ν as determined from the fitting of optical model cross sections was found to be 1.15 for protons and 1.32 for α particles. It was assumed to be 1.32 for all other clusters, in the absence of a global optical model parameter set with which to compare SCO results.

D. Transmission coefficients for deformed nuclei

A qualitative consideration of the problem of evaporation from a deformed rather than spherical system is useful. Classically, $l_m = \vec{R} \times \vec{P}$; then l_m for neutron emission from the tip of a deformed nucleus leads to twice the result of a spherical nucleus if the deformed nucleus major axis is twice that of the spherical nucleus (which according to the RLD model is the case for many nuclei formed in heavy ion reactions). However, some emission will take place from the "waist" region of the deformed nucleus, leading to lower l_m than for the spherical system. Clearly an averaging must be performed; the evaporation aspect suggests that the weighting be proportional to the surface area. The qualitative argument is similar for charged particle emission, except that in this case l_m depends not only on radius of emission,

TABLE I. Barriers, deformation, and maximum orbital angular momenta versus compound nucleus angular momentum for ^{56}Ni and ^{148}Sm.

Emitting nucleus	Angular momentum ($\hbar$)	R_{maj}[a]	R_{min}[a]	V/V_0[b] (MeV)	Ejectile: p		α		^{6}Li		^{7}Li		^{8}Be		^{9}Be		^{10}B		^{12}C	
				Ejectile energy (MeV):	20	40	20	40	20	40	20	40	20	40	20	40	20	40	20	40
					Maximum orbital angular momenta ($\hbar$)															
^{56}Ni	5	1.00	1.00	1.0	7	10	11	18	12	22	13	24	11	24	11	25	8	25	0	26
	25	1.07	0.87	0.97	7	10	12	19	12	23	14	25	12	25	12	27	9	26	5	27
	35	1.22	0.90	0.91	8	12	13	21	14	25	15	27	14	28	14	29	12	29	8	30
	45	1.79	0.75	0.72	12	17	19	29	21	34	22	37	21	38	23	40	21	40	19	42
	55	2.20	0.67	0.62	14	21	23	35	26	41	28	44	27	46	28	48	27	49	28	44
^{148}Sm	5	1.00	1.00	1.0	8	12	7	21	0	22	0	24	0	18	0	20	0	6	0	0
	75	1.08	0.85	0.96	8	13	9	23	0	24	0	26	0	21	0	22	0	11	0	0
	85	1.52	0.81	0.80	12	18	15	31	0	34	0	37	0	33	0	36	0	29	0	18
	95	2.13	0.69	0.63	17	26	24	44	20	49	22	54	0	51	0	55	0	50	0	46

[a] Ratio of major (maj) or minor (min) axis to radius of spherical nucleus.
[b] Ratio of Coulomb barrier at surface along major axis to Coulomb barrier of spherical nucleus.

but on the barrier height at the point on the surface from which emission takes place [see Eqs. (6) and (7)]. This barrier height differs from that of the spherical nucleus due to both the nonspherical matter and the nonspherical charge distributions.

For neutrons, the $T_l(\epsilon)$ were computed averaged over 50 "slices" of the nucleus along the symmetry axis with the R of Eq. (5) replaced by the distance from the center to the surface point (ring) of emission. The nuclei were assumed to be ellipsoids of revolution, with the major axis given by the RLD model, and the minor axis determined by volume conservation. Figures showing representative T_l sets for deformed nuclei were presented in (7).

For charged particles the procedure was similar to that for neutrons, except that the V_ν of Eqs. (6) and (7) as well as the R had to be recomputed for each ring of the nuclear surface. The equations describing these computations are to be found in (7). The deformations at each angular momentum were computed according to the RLD model; the R, but not the R_ν were modified for deformation as indicated.

In the remainder of this work we will consider results of the deexcitation of ^{56}Ni at 176 and 96 MeV of excitation, and of ^{148}Sm at 135 MeV of excitation. These choices were made in order to show results for the rare earth and for a light mass system. In Table I the relevant deformations to be expected versus compound nucleus angular momentum are summarized, as well as l_m for several channel energies for the protons and clusters considered. The large increase in l_m with deformation (angular momentum) may be seen in Table I, especially for the clusters.

E. Population of superdeformed nuclei

It is worthwhile to indicate the expected fraction of the compound nucleus cross section which may be populated in the superdeformed nucleus region. This mass dependent function is shown in Fig. 2, where the relative cross sections which could be populated in the spherical/oblate region vs the prolate/triaxial regions are indicated versus mass number (based on the RLD model). The RLD limit for cross sections (which should be proportional to J^2) above which the fission barrier is zero is also indicated in Fig. 2. Finally, the ratio of prolate/triaxial nuclei to spherical/oblate nuclei (according to the RLD model) versus mass number is shown. As an example of the use of Fig. 2 we consider mass number 80. A vertical line through 80 (abscissa) intersects the solid line at a relative cross section (J^2) of 2000 units. The fission barrier disappears (becomes equal to zero) at

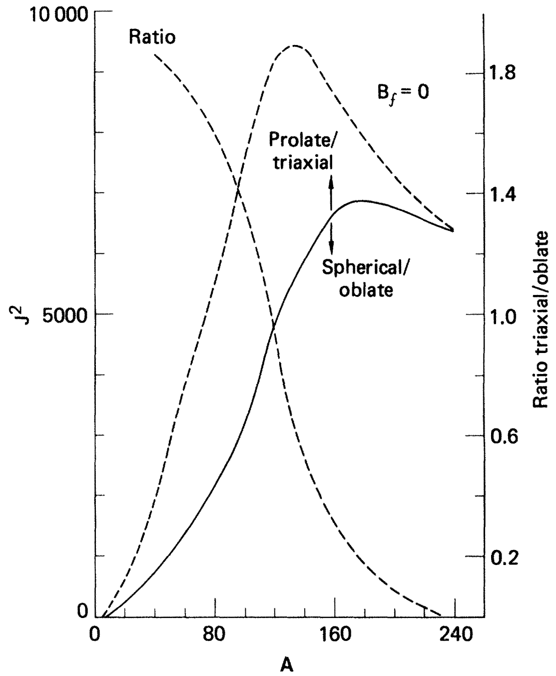

FIG. 2. Relative cross section limits and ratios for populating spherical/oblate versus prolate/triaxial nuclei as function of mass number according to the rotating liquid drop model. The left ordinate is the square of the angular momentum quantum number of the rotating nucleus; the right ordinate is for the ratio curve. Mass number is given on the abscissa. The solid curve represents the transition between spherical/oblate (S/O) and prolate/triaxial (P/T) nuclei; cross section (proportional to J^2) below the solid curve represents the S/O limit, whereas the cross section above the solid curve represents the P/T result. The loci of angular momenta (squared) for which the RLD fission barrier is predicted to vanish is shown as a dashed line. The ratio of cross sections above the S/O-P/T transition line and below the $B_f = 0$ line, to those below the transition line are shown as the ratio line.

$J^2 = 5500$ units. Then 2000 units of cross section may be populated by spherical and oblately deformed nuclei, and $5500 - 2000 = 3500$ units as prolate and triaxially deformed nuclei. The ratio of the latter to the former is approximately 1.7 : 1, as given by the curve labeled "ratio." It may be seen that a major portion of compound cross sections may be superdeformed over a wide range of masses. (Some preliminary experimental results suggest an onset of prolate shapes at even lower angular momenta than predicted by the RLD model.[15]) It is obvious that these deformed shapes must not be overlooked in reaction models. It is the purpose of this work to indicate how the deexcitation of these highly deformed nuclei might be expected to differ from earlier statistical decay models.

F. Uncertainties in model

Model calculations are no better than the parameters and/or approximations used. We therefore give some discussion of these points to emphasize that the results of these calculations are more a qualitative guide to the types and directions of deviations expected from earlier statistical model results than quantitative predictions to be quoted verbatim and tested quantitatively. The model calculation can, of course, also be irrelevant if the physical assumptions are incorrect, or the reaction mechanism different than that assumed.

The most crucial factors in the modeling decay of highly deformed nuclei is in the computation of $T_l(\epsilon)$ and the evaluation of the related yrast energies. Sources of error in T_l result from uncertainties in the accuracy of the liquid drop shapes versus I, and in the parametrizations assumed in replacing the R and V of Eqs. (5)–(7) with deformed radii and in the averaging used. The question of yrast energies is, we think, open to controversy, and we therefore have chosen to explore several limits as described in Sec. II B.

Simplification in using Eq. (1) comes about from taking the intrinsic particle spin out of the summation as a multiplicative constant $(2S_\nu + 1)$. For neutrons and protons this should be a very good approximation. For ^{7}Li, ^{9}Be, and ^{10}B with spin 3, this may overestimate their emission rates. This overestimation should have an upper limit of a factor of 3, and is probably much less. Another more important question than the factorization of the spin degeneracy is the physical question of decay prior to the attainment of equilibrium. The increased emission rates from deformed nuclei over spherical nuclei would imply this possibility, and this would alter branching ratios. With these reservations in mind, we next consider comparisons of statistical model results for deexcitation of spherical versus deformed nuclei.

III. RESULTS

A. General model predictions

Decay characteristics for the ^{56}Ni and ^{148}Sm compound nuclei are summarized in Tables II–IV and in Figs. 3–5. An interesting quantity to define and compare is the ratio of emission rates for either a particular ejectile or for all ejectiles when deformation is considered for T_l [calculations (B), (C), and (D)] to the case where it is not [calculation (A)]. We refer to this ratio as the amplification factor,

TABLE II. Decay probabilities and amplification factors for ^{56}Ni nuclei at 176 MeV excitation energy.

Compound nucleus angular momentum ($\hbar$)	54				50			
Calculation	(A)	(B)	(C)	(D)	(A)	(B)	(C)	(D)
Fractional decay								
f_f	0.35[a]	5.4(−3)[b]	0.141	0.23	0.23	3.7(−3)	0.180	0.152
f_n	0.106	1.6(−3)	0.110	0.063	0.047	1.7(−3)	0.068	0.051
f_p	0.26	7.8(−3)	0.33	0.30	0.20	8.2(−3)	0.33	0.24
f_α	0.145	0.069	0.33	0.25	0.20	0.13	0.33	0.28
$f_{^{12}C}$	0.090	0.56	0.036	0.092	0.20	0.48	0.037	0.17
$f_{^7\mathrm{Li}}$	8.9(−4)	9.1(−3)	1.7(−3)	1.7(−3)	2.9(−3)	0.012	1.9(−3)	3.2(−3)
$f_{^8\mathrm{Be}}$	0.032	0.21	0.042	0.047	0.083	0.23	0.044	0.082
$f_{^9\mathrm{Be}}$	2.4(−3)	0.029	2.1(−3)		7.3(−3)	0.031	2.4(−3)	7.1(−3)
$f_{^{10}\mathrm{B}}$	9.0(−3)	0.11	6.4(−3)	0.011	0.026	0.11	7.0(−3)	0.024
Amplification factors:								
All particles		100	3.3	1.8		84	1.4	1.7
α		30	5.7	2.6		40	2.1	2.1
^{12}C		400	1.0	1.5		150	0.2	1.3
^{8}Be		430	3.3	2.2		170	0.7	1.7
^{10}B		790	1.8	1.8		260	0.34	1.7

[a] Fission calculated for $a_f/a_\nu = 1.03$ and fission barriers 0.6 times RLD values.
[b] Numbers in parentheses are exponents base 10.

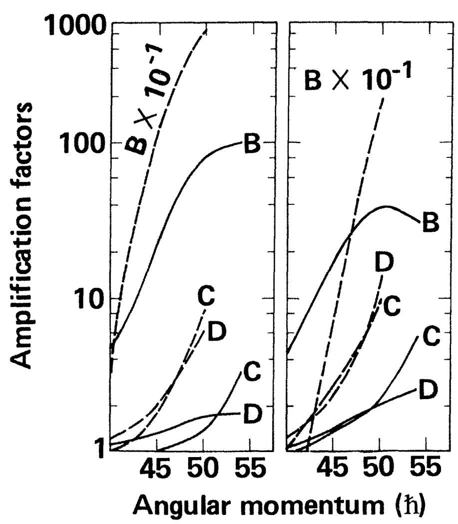

FIG. 3. Total and alpha particle amplification factors versus angular momentum for ^{56}Ni nuclei at 95 and 176 MeV for calculations (B)–(D). Total factors are shown in the left half of figure.

$$A = \frac{R_i^D}{R_i^S} = \frac{f_f^S}{f_f^D} \cdot \frac{f_i^D}{f_i^S}, \tag{8}$$

where R_i^D represents the emission rate from the deformed nucleus [calculations (B), (C), or (D)] and R_i^S the rate from the spherical T_l calculation

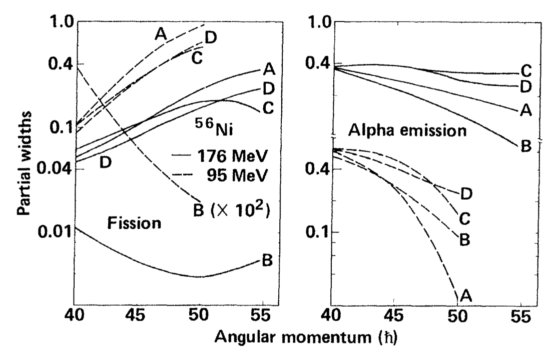

FIG. 4. Partial decay widths for fission and alpha emission versus compound nucleus angular momentum for ^{56}Ni nuclei at 95 MeV (dashed line) and 176 MeV (solid line) excitation. The four types of calculations are described in the text.

TABLE II. (*Continued*).

45				40				5
(A)	(B)	(C)	(D)	(A)	(B)	(C)	(D)	(A)
0.106	5.3(−3)	0.107	0.082	0.052	0.011	0.062	0.047	1.7(−3)
0.040	4.7(−3)	0.066	0.046	0.044	0.017	0.073	0.048	0.26
0.16	0.020	0.29	0.20	0.17	0.065	0.29	0.18	0.47
0.27	0.23	0.39	0.30	0.37	0.35	0.41	0.37	0.22
0.23	0.38	0.059	0.20	0.17	0.25	0.063	0.16	6.6(−3)
6.2(−3)	0.015	3.7(−3)	6.2(−3)	3.6(−3)	0.014	5.1(−3)	8.7(−3)	5.3(−3)
0.13	0.23	0.067	0.12	0.13	0.19	0.075	0.13	0.018
0.013	0.030	4.7(−3)	0.012	0.015	0.025	6.3(−3)	0.014	3.7(−3)
0.041	0.098	0.013	0.038	0.041	0.072	0.017	0.040	4.1(−3)
	22	1.0	1.3		4.9	0.8	1.1	
	17	1.4	1.4		4.5	1.0	1.1	
	33	0.3	1.1		6.9	0.3	1.0	
	35	0.5	1.2		6.9	0.5	1.10	
	48	0.3	1.2		8.3	0.4	1.08	

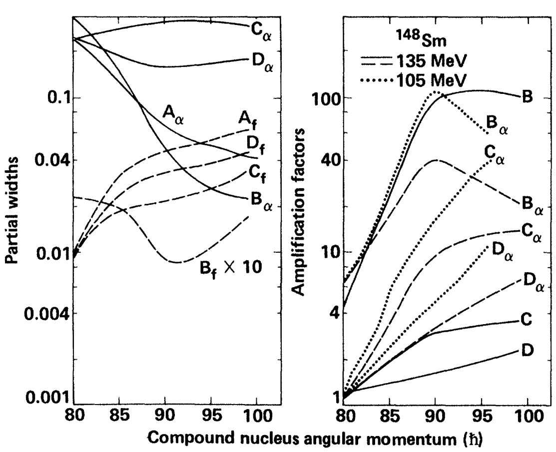

FIG. 5. Partial widths and amplification factors for total and α particle emission versus angular momentum for ^{148}Sm nuclei at 105 and 135 MeV excitation. Calculations (B)–(D) are described in the text. Partial decay widths for fission are also shown. Subscripts denote α or fission (f) widths.

(A); f_f represents the calculated fractional decay by fission from the deformed or spherical nucleus, and f_i is the corresponding fractional emission of particle i. These decay fractions and many amplification factors are summarized in Tables II–IV.

Consider first the ^{56}Ni systems (Tables II and III; Figs. 3 and 4). For the standard calculation (A), the fission probabilities are negligible at low angular momenta, becoming significant at angular momenta above $40\hbar$. Neutron, proton, and α decay are the main channels at lower angular momenta. At higher angular momenta some significant evaporation of ^{12}C and ^{8}Be is predicted even in calculation (A). When the extreme formulation (B) is applied, very large particle emission amplification factors result (Fig. 3). This leads to large predicted enhancements of cluster emission for α, ^{12}C, ^{8}Be, and ^{10}B, with all these expected to constitute a substantial fraction of the first chance decay cross sections.

When the more reasonable calculations (C) and (D) are considered the following should be noted:

(i) Total particle emission amplification factors

TABLE III. Decay probabilities and amplification factors for ^{56}Ni nuclei at 94 MeV excitation energy.

Compound nucleus angular momentum $\hbar$	50				45				40				5
Calculation	(A)	(B)	(C)	(D)	(A)	(B)	(C)	(D)	(A)	(B)	(C)	(D)	(A)
Fractional decay:													
f_f	0.92[a]	1.9(−4)[b]	0.58	0.65	0.43	6.4(−4)	0.300	0.28	0.110	3.7(−3)	0.110	0.089	6.0(−4)
f_m	5.1(−4)	9.4(−7)	1.1(−3)	9.9(−4)	3.6(−3)	3.8(−5)	5.4(−3)	4.9(−3)	8.1(−3)	9.2(−4)	0.015	9.5(−3)	0.23
f_p	0.0227	4.7(−5)	0.066	0.054	0.076	8.7(−4)	0.144	0.1132	0.106	0.013	0.21	0.122	0.55
f_α	0.0244	0.095	0.15	0.24	0.27	0.27	0.50	0.408	0.60	0.53	0.62	0.61	0.22
f_c	0.032	0.61	0.19	0.046	0.144	0.43	0.027	0.126	0.090	0.23	0.013	0.083	6.9(−4)
$f_{^7\mathrm{Li}}$		4.4(−4)	1.8(−6)		3.0(−6)	7.9(−4)	2.0(−6)	6.7(−6)	6.2(−5)	8.1(−4)	2.2(−5)	7.9(−5)	3.0(−4)
$f_{^8\mathrm{Be}}$	5.1(−3)	0.28	0.013	0.013	0.070	0.28	0.18	0.070	0.089	0.22	0.029	0.088	4.7(−3)
$f_{^9\mathrm{Be}}$		1.6(−3)	7.1(−5)		1.8(−5)	1.9(−3)	1.8(−5)	2.4(−5)	1.2(−4)	1.4(−3)	2.0(−5)	1.3(−4)	1.1(−4)
$f_{^{10}\mathrm{B}}$		0.018	1.7(−3)	9.9(−6)	3.3(−4)	0.017	3.8(−4)	4.1(−4)	1.1(−3)	0.010	2.0(−4)	1.1(−3)	1.8(−4)
Amplification factors:													
All particles		5.3(1+3)	8.3	6.2		1.2(+3)	1.8	1.9		30	1.00	1.3	
α		1.9(+4)	9.8	14		6.7(+2)	2.7	2.3		30	1.0	1.2	
^{12}C		9.1(+4)	9.4	2.0		2.0(+3)	0.3	1.4		80	0.14	1.1	
^{8}Be		2.6(+5)	4.1	3.6		2.7(+3)	0.4	1.5		70	0.3	1.2	
^{10}B						3.5(+4)	1.7	1.9		270	0.2	1.2	

[a] Fission calculated for $a_f/a_\nu = 1.03$ and fission barriers 0.6 times RLD values.
[b] Numbers in parentheses are exponents base 10.

of 2–3 result at 176 MeV excitation, and factors of 6–7 result at 96 MeV. This shows a significant increase of particle emission amplification with decreasing excitation such as, e.g., following successive neutron emission. These emission rate increases may be important in deducing fission parameters by fitting fission and evaporation residue excitation functions.

(ii) The observations of (i) hold true for the α particle amplification factors, which tend to be larger than the total particle emission amplification factors (Fig. 3). The particle emission amplifications noted lead to a decrease in fission probability at the higher angular momenta and an increase in α emission. These effects should become more pronounced for lower compound nucleus excitations or in secondary decay of residual nuclei following primary particle evaporation.

It should be noted that calculation (C) can lead to decreased emission rates for heavy clusters for some compound nuclei. Reasons for this may be seen by reference to Fig. 1 (note the decrease in effective excitation above the yrast line for frozen compound nucleus deformation). Consider next Table IV and Fig. 5 for decay of ^{148}Sm nuclei at 135 MeV of excitation. Here neutron emission is the principal decay channel at all but the highest angular momenta for the standard calculation (A). Fission becomes the dominant channel at the highest angular momenta; alpha particle emission is significant over a part of the angular momentum range; no other clusters contribute significantly. If one goes to the extreme calculation (B), one finds very large amplification factors for cluster emission with resultant suppression of fission at the higher angular momenta. The result is a prediction that ^{8}Be and ^{12}C are the most probable first chance ejectiles for compound nuclei between 85 and 100 $\hbar$.

Calculations (C) and (D) predict overall particle emission amplification of factors of 2-4, which (as for ^{56}Ni) may be significant for determination of liquid drop fission parameters from experimental data. It may be seen that the predicted fission probabilities decrease significantly even for the more conservative assumptions [calculations (C) and (D)]; the α amplification factors exceed a factor of 10 for (C) and a factor of 5 for (D). At lower excitations, as for ^{56}Ni, these factors become still larger [e.g., 40 for (C) and 10 for (D) at 95$\hbar$ and 105 MeV]. They are therefore expected to raise the α particle emission probabilities to significant levels for first chance emission, with significant probabilities for emission following neutron evaporation. Amplification factors for ^{12}C and ^{10}B are of the order of 10^3 for (C) and 50 for (D). This leads to a prediction that the highest angular momentum compound nuclei might deexcite initially by emission of heavy clusters; the residual nuclei would in many cases still have sufficiently high angular momenta to undergo fission.

B. Alpha particle evaporation spectra

It is instructive to compare the α spectra predicted by formulations (A)–(D) for the two mass systems under discussion. These results are shown in Fig. 6 for ^{148}Sm at 90$\hbar$ and for ^{56}Ni at 50$\hbar$. A major part of the α particle amplification for calculations (C) and (D) may be seen to come from the decrease in Coulomb barrier due to the high deformations, as shown by the enhancement of low energy α particles relative to the spherical nucleus calculation (A). Such an effect has been seen, and the mechanism has been suggested by Logan *et al.*[16] It is the presence of the low energy ("sub-barrier") α group which leads to a decrease in the average kinetic energy for calculations (C) and (D) versus (A) (17.1 MeV versus 19.6 MeV) and to a slightly lower average angular momentum removal for (D) than (A) (3.6$\hbar$ versus 3.9$\hbar$). Calculation (C), due to using T_l based on the compound nucleus deformation, is predicted to show an average angular momentum decrement of 8.8$\hbar$, in contrast to the other two cases.

The extreme calculation (B) yields an average kinetic energy of 23.6 MeV and angular momentum decrement of 20.2$\hbar$. Here the main amplification comes from high energy α particle emission rather than sub-barrier emission This is the result of the rate at which the maximum value of l changes with the ejectile kinetic energy versus decrease in energy of the yrast line when the compound nucleus

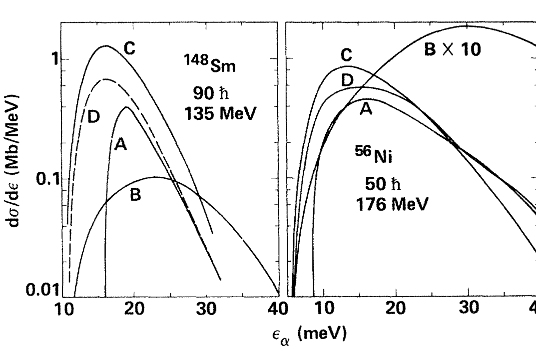

FIG. 6. Alpha particle spectra predicted for decay of ^{148}Sm nuclei of 90$\hbar$ and 135 MeV excitation and ^{56}Ni nuclei of 50$\hbar$ and 176 MeV excitation. Calculations (A)–(D) are described in the text.

TABLE IV. Decay probabilities and amplification factors for ^{148}Sm nuclei at 135 MeV excitation energy.

Compound nucleus angular momentum $\hbar$	98				95			
Calculation	(A)	(B)	(C)	(D)	(A)	(B)	(C)	(D)
Fractional decay:								
f_f[a]	0.64	0.017	0.33	0.44	0.54	0.0105	0.26	0.38
f_n	0.31	1.4(−3)[b]	0.29	0.35	0.39	0.013	0.35	0.42
f_p	8.1(−3)	6.7(−4)	0.014	0.016	0.011	2.0(−3)	0.016	0.019
f_α	0.040	0.023	0.29	0.18	0.050	0.026	0.31	0.17
$f_{^{12}\mathrm{C}}$	5.1(−5)	0.80	0.035	2.0(−3)	1.1(−4)	0.78	0.040	1.5(−3)
$f_{^{7}\mathrm{Li}}$	1.7(−5)	3.7(−3)	2.1(−3)	5.3(−4)	6.7(−5)	4.7(−3)	2.5(−3)	4.8(−4)
$f_{^{8}\mathrm{Be}}$	3.1(−4)	0.11	0.033	6.2(−3)	4.5(−4)	0.12	0.037	5.2(−3)
$f_{^{9}\mathrm{Be}}$	2.2(−5)	0.026	3.2(−3)	4.3(−4)	3.8(−5)	0.030	3.8(−3)	3.7(−4)
$f_{^{10}\mathrm{B}}$	1.1(−6)	0.013	7.0(−4)	5.4(−5)	2.4(−6)	0.014	8.5(−4)	4.3(−5)
Amplification factors:								
All particles		100	3.6	2.3		110	3.3	1.9
α		21	14	6.4		27	13	48
^{12}C		2.6(+4)	1330	58		2.0(+5)	830	19.4
^{8}Be		1.3(+4)	190	29		1.4(+4)	170	16
^{10}B		4.9(+5)	1360	73		3.1(+5)	740	25

[a] Calculated for $a_f/a_\nu = 1.0$ and RLD fission barriers.
[b] Numbers in parentheses are exponents base 10.

deformation is used for T_l and the equilibrium residual nucleus shape is used for the yrast calculation. The predicted kinetic energy spectra may be seen to be sensitive to the interrelations of these two quantities. Conclusions for the α spectra from ^{56}Ni are similar to those for ^{148}Sm; the physical effects of the different formulations are qualitatively the same, with some quantitative differences as may be seen in Fig. 6.

The general conclusions as to the effects presented to this point are for significant overall increases in particle emission rates versus fission when deformation is considered. Alpha particle emission rates are always predicted to be enhanced, and heavier cluster emission is also enhanced in most cases. These effects should be more pronounced at lower excitations, and even in the most conservative formulations should be sizable corrections to evaporation expectations as generally formulated.

C. Qualitative comparisons with experimental observations

Oeschler *et al.* have recently measured fission fragment yields and Z distributions for the system ^{30}Si + ^{132}Xe at bombarding energies of 5.4 to 8.2 MeV/A (lab) for the ^{132}Xe projectile.[17] A symmetric fission group was observed which had its peak at half the compound nucleus Z at 5.4 MeV/A incident ^{132}Xe energy. As the bombarding energy was increased, the centroid moved to a value characteristic of fission of a nucleus 4 units lower in charge. This is consistent with the results presented in Table IV for the extreme calculation, where first chance fission rapidly decreases and evaporation of $Z = 2-6$ clusters rapidly increases with increasing angular momenta; it is in rough agreement with the more conservative results [(C) and (D)] when the contribution of multiple α emission is also considered. The increasing bombarding energies, of course, produce an increase in the spin distributions of compound nuclei; the onset of the shift in Z in the yields of Ref. 17 corresponds to the bombarding energy at which significant cross sections for superdeformed compound nuclei are predicted. Application of the old statistical model approach would require a direct reaction interpretation of the results cited. The new model permits an equilibrium inter-

TABLE IV. *(Continued)*.

90				85				80			
(A)	(B)	(C)	(D)	(A)	(B)	(C)	(D)	(A)	(B)	(C)	(D)
0.46	9.3	0.22	0.34	0.31	0.020	0.19	0.24	0.097	0.023	0.088	0.082
0.45	0.014	0.37	0.47	0.53	0.055	0.49	0.54	0.62	0.21	0.62	0.62
0.013	6.8(−4)	0.018	0.019	0.017	2.4(−3)	0.021	0.020	0.021	8.8(−3)	0.025	0.022
0.067	0.048	0.31	0.16	0.13	0.15	0.27	0.19	0.24	0.34	0.24	0.254
5.0(−4)	0.73	0.033(−2)	1.4(−3)	2.0(−3)	0.54	0.012(−2)	2.7(−3)	3.9(−3)	0.23	5.4(−3)	4.6(−3)
1.8(−4)	6.8(−3)	2.5(−3)	5.1(−4)	7.2(−4)	0.011	1.7(−3)	9.5(−4)	1.8(−3)	0.012	1.4(−3)	1.9(−3)
1.3(−3)	0.14	0.034	4.6(−3)	4.9(−3)	0.17	0.018	7.4(−3)	0.011	0.14	0.012	0.013
1.6(−4)	0.035	3.7(−3)	4.0(−4)	7.1(−4)	0.037	2.0(−3)	8.9(−4)	1.7(−3)	0.027	1.3(−3)	1.8(−3)
1.3(−5)	0.015	8.0(−4)	4.2(−5)	6.6(−5)	0.013	3.4(−4)	8.9(−5)	1.6(−4)	6.9(−3)	1.8(−4)	1.9(−4)
	95	3.0	1.7		22	1.9	1.4		4.4	1.1	1.2
	40	9.7	3.2		18	3.2	1.9		6.0	1.1	1.2
	7.5(+4)	140	4.0		6.0(+3)	10.0	1.7		250	1.5	1.4
	5.5(+3)	55	5.0		540	6.0	2.0		80	1.2	1.4
	1.8(+4)	129	4.4		3.0(+3)	13	1.8		180	1.2	1.4

pretation which seems more consistent with other measurements of reaction mechanisms in this energy range (~1.2 MeV/A center of mass). Angular distribution measurements of the charged particles emitted in coincidence with the fission fragments in this experiment would be valuable in deciding this question.

It has been pointed out that the proposed cluster amplification mechanism is consistent with experimental results presented by Britt *et al.*[18] and recent results of Hillis *et al.*[19] Both sources reported on γ-ray multiplicity measurements in the evaporation residue (ER) compound nucleus region. A conclusion was that evaporation residue products could not be produced with $J > 65\hbar$. On the other hand, ER cross section measurements suggested higher values of angular momenta contributing to the ER cross section (however, these experimental results had large uncertainties and would best be repeated to higher precision). These two apparently contradictory J limits for ER formation are consistent with cluster decay amplification, as quite high l waves may accompany cluster emission, giving an ER cross section at lower J which can then survive fission decay. These residual ER would show a γ-ray multiplicity characteristic of a much lower J than the original compound nuclei, having been populated by compound nuclei originally formed at higher J, but deexciting to ER at considerably lower angular momenta.

Many additional experimental results which are consistent with the proposed cluster emission amplification mechanism have been summarized in Ref. 7. An additional result comes from the Marburg/GSI group; they have investigated reaction yields versus bombarding energy for the system $^{46}Ti + ^{24}Mg$.[20] At the lower bombarding energies (below 4.7 MeV/A) the final product yields were in excellent agreement with standard HF statistical model calculations. However at energies in the range of 5.8 to 8.5 MeV/A (for which large superdeformed nucleus cross sections are expected), the experimental results showed far higher yields of products which could be populated by emission of three or more α particles (or by other clusters). While this was tentatively interpreted by the authors as evidence for a preequilibrium mechanism, it may also be seen from Fig. 3, and Tables I–III that it is also consistent with compound nucleus evaporation when superdeformation is considered. We further note that significant precompound decay of the intrinsic excitation type at such low bombarding energies would be unexpected.

Attention should be drawn to an earlier work of Pühlhofer *et al.*[21] who measured product yields for the reaction $^{24,25,26}Mg + ^{32}S$ at 160 MeV. They also found final products which corresponded to enhanced α particle emission. The possibly important role of deformation on $T_l(\epsilon)$ was pointed out in this work, and a calculation using optical model $T_l(\epsilon)$ generated assuming a 10% radius increase was performed. It was found that the predicted yields of the latter calculation were in better agreement with the experimental yields than was the standard calculation.

It should be pointed out that the cluster emission amplification mechanism has important implications for the interpretation of various experiments investigating the maximum angular momentum for fusion (l_{max}). Measurements have often been made of the sum of evaporation residue plus fission cross sections. The l_{max} deduced from this sum has in some cases exceeded the predicted liquid drop limit.[22] However, the rapid increase of cluster emission probability and resulting decrease of fission probability means that the rate at which clusters can be emitted may far exceed the rate of fission. Cluster emission amplification in the extreme case results from the exponential phase space increase accessible from mostly antiparallel coupling of composite system and ejectile orbital angular momenta which may be due to the large radii of the superdeformed nuclei (see Table I). This can result in residual nuclei of 10–20 $\hbar$ lower angular momentum following first chance α emission, and still lower values when heavier ejectiles are involved. Therefore, while there may be no fission barrier in the initial composite system, residual nuclei which do have a fission barrier could be formed prior to fission due to cluster amplification decay from an equilibrated or quasiequilibrated system. Precompound master equation calculations predict particle emission during coalescence,[23,24] and there is experimental evidence for this phenomenon as well. This would lead to a broadening in the fission yield curve (since many different daughter nucleides may be undergoing fission) but a more likely explanation for the experimentally observed broadening (if such yields are indeed from equilibrium fission) would be less stiffness to asymmetry as the fission barrier decreases.[25]

The question of applying the deformed nucleus amplification mechanism to quasiequilibrium systems is worth a qualitative exploration. It has been shown that there is an equilibration of excitation energy even in deep inelastic reactions.[26-28] Particle-hole degrees of freedom should either equilibrate or go far towards equilibrium on a time scale close to the coalescence period. Direct reaction models contain a final state component. In this case the residual nucleus level density and ejectile phase space factors may represent the final state. If the final state density is not fully equilibrated, it may well be closely proportional to the equilibrated value. But if as in the calculations of this work, the collective deformation and rotational energy of the final nucleus is an important aspect of the final state, then the model predictions of this work should be relevant to nonequilibrium reactions as well, except that the ejectiles should be forward peaked rather than symmetric about 90°. This idea may be relevant in the interpretation of the $^{160}Gd(^{12}C, \alpha x n)$ and $(^{12}C, 3\alpha)$ reactions recently reported by Wilczynski and co-workers, although these results seem to be more characteristic of direct reactions as interpreted by the authors.[29,30]

Worthwhile future experiments would include searches for cluster emission with projectiles heavier than ^{12}C (less prone to fragmentation than ^{12}C) at lower incident energies. One wants reactions with a large population of superdeformed nuclei produced with projectiles not prone to fragmentation or breakup; as mentioned earlier a "gate" on decay of higher angular momentum states would aid such experimental measurements. Such a gate might be on high total γ-decay energy or on fission fragments.

IV. CONCLUSIONS

Figure 2 illustrates that a major fraction of heavy ion reaction yields may, according to the RLD model, populate highly deformed triaxial nuclei ("superdeformed nuclei"). Comparisons have been made between HF-type decay calculations in which transmission coefficients for particle decay were used for spherical nuclei (as has been standard practice) and several sets of calculations for which particle emission transmission coefficients were modeled for deformed nuclei, with deformations as given by the RLD model.

The comparisons show a predicted new decay mechanism which has been called cluster decay amplification (for fully equilibrated systems) or centrifugal fragmentation (for quasiequilibrated systems) after a consideration of its causes. The quantitative degree to which nature may agree with the computer modeling remains to be shown; it will depend very much on how realistically the $T_l(\epsilon)$ have been modeled for the deformed nuclei and on the reaction dynamics. The results presented herein should therefore be interpreted as qualitative suggestions of deviations between "new" and "old" statistical model approaches rather than as quantitative predictions.

Many experimental observations in heavy ion reactions are consistent with the proposed new mechanisms; it would permit an equilibrium interpretation to be placed on many phenomena which heretofore had been interpreted as noncompound or precompound. However, we feel that experiments to date provide only circumstantial evidence for cluster amplification; more direct experiments have been suggested.

Nuclear physics has long been involved in the investigation of limits of nuclear matter. One important such frontier area is nuclear matter at very large deformations. It may provide the basis for understanding important collective variables in many heavy ion induced "direct" reactions which may be described in a sort of quasiequilibrium fashion. The area is a potentially valuable and fruitful one for further and deeper investigation. Whether the potential will be realized when nature renders the answers remain to be seen.

ACKNOWLEDGMENTS

The authors have appreciated helpful discussions with Professor R. Vandenbosch [who suggested approach (C)] and with Professor L. G. Moretto and Professor A. Kermin. This work was performed under the auspices of the U. S. Department of Energy by Lawrence Livermore Laboratory under Contract No. W-7405-ENG-48.

---

[1]S. Cohen, F. Plasil, and W. J. Swiatecki, Ann. Phys. (N.Y.) 82, 557 (1974).
[2]F. Plasil and M. Blann, Phys. Rev. C 11, 508 (1975).
[3]M. Beckerman and M. Blann, Phys. Rev. C 17, 1615 (1978).
[4]J. Bisplinghoff *et al.*, Phys. Rev. C 16, 1058 (1977).
[5]M. Beckerman and M. Blann, Phys. Rev. Lett. 42, 156 (1979).
[6]M. Blann, Phys. Lett. 88B, 5 (1979).
[7]M. Blann, Phys. Rev. C 21, 1770 (1980).
[8]M. Beckerman and M. Blann, University of Rochester Report No. UR-NSRL-135A, 1977 (unpublished); M. Blann, Phys. Rev. 157, 860 (1967).
[9]D. W. Lang, Nucl. Phys. 77, 545 (1966).
[10]L. G. Moretto, Nucl. Phys. A247, 211 (1975).
[11]M. Blann and F. Plasil, University of Rochester Report No. C00-3494-10, 1973 (unpublished); M. Blann, University of Rochester Report No. C00-3494-29 (1976).
[12]D. Wilmore and P. E. Hodgson, Nucl. Phys. 55, 673 (1964).
[13]F. G. Perey, Phys. Rev. 131, 745 (1963).
[14]G. R. Satchler, Nucl. Phys. 70, 177 (1965).
[15]R. M. Diamond, private communication.
[16]D. Logan *et al.*, Phys. Rev. C 22, 104 (1980).
[17]H. Oeschler *et al.*, Phys. Rev. C 22, 546 (1980).
[18]H. C. Britt *et al.*, Phys. Rev. Lett. 18, 1164 (1978).
[19]D. L. Hillis *et al.*, GSI progress Report No. GSI 79-11, 1979, p. 28 (unpublished).
[20]B. Kohlmeyer *et al.*, GSI progress Report No. GSI 79-11, 1979, p. 5 (unpublished).
[21]F. Pühlhofer *et al.*, Phys. Rev. C 16, 1010 (1977).
[22]M. Lefort, Symposium on Heavy Ion Fusion Reactions, Bad Honnef, 1980; Orsay Report No. IPNO-RC-80-03 (unpublished).
[23]M. Blann and M. Beckerman, Nukleonika 23, 1 (1978).
[24]M. Blann, A. Mignerey, and W. Scobel, Nukleonika 21, 335 (1976); M. Blann, Phys. Rev. C 23, 205 (1981).
[25]C. Gregoire *et al.*, Saclay Report No. DPL-N/MF/79/33, 1979 (unpublished).
[26]F. Plasil *et al.*, Phys. Rev. Lett. 40, 1164 (1978); M. Blann *et al.*, Phys. Rev. 19, 1288 (1979).
[27]B. Tamain *et al.*, Orsay Report No. IPNO-RC-79-02, 1979 (unpublished).
[28]Y. Eyal *et al.*, Phys. Rev. Lett. 41, 625 (1978).
[29]K. Siwek-Wilczynski *et al.*, Phys. Rev. Lett. 42, 1599 (1979).
[30]J. Wilczynski *et al.*, Gröningen Report No. KVI-193, 1979 (unpublished); K. Siwek-Wilczynska *et al.*, Gröningen Report No. KVI-174, 1979 (unpublished).